

Infrared spectra, optical constants and semiconductor behavior of 5-(2-phenylhydrazono)-3,3-dimethylcyclohexanone thin films

E.M. El-Menyawy^{a,*}, N.A. El-Ghamaz^b, H.H. Nawar^c

^a Solid State Electronics Laboratory, Solid State Physics Department, Physics Division, National Research Center, Dokki, Cairo 12615, Egypt

^b Department of Physics, Faculty of Science at New Damietta, Damietta University, 34517 New Damietta, Egypt

^c Department of Chemistry, Faculty of Education, Al-Jabl Al Gharbi University, Libya

HIGHLIGHTS

- ▶ Hydrazine derivative has been synthesized.
- ▶ FTIR indicates that the thermal evaporation is suitable technique for obtaining thin films.
- ▶ Optical constants of thin films are independent of their thickness.
- ▶ The compound has semiconductor behavior.

ARTICLE INFO

Article history:

Received 7 July 2012

Received in revised form 25 August 2012

Accepted 25 September 2012

Available online 2 October 2012

Keywords:

Organic thin films
Structural properties
Optical constants
Conductivity

ABSTRACT

The 5-(2-phenylhydrazono)-3,3-dimethylcyclohexanone (PHDMC) is synthesized by reacting 5,5-dimethylcyclohexane-1,3-dione with 2-phenylhydrazine. Synthesized PHDMC is polycrystalline with monoclinic space group, $P2_1/a$. Miller's indices values for each diffraction peak in the X-ray diffraction spectrum are calculated. Thin films of PHDMC with different thickness values (0.83–1.247 μm) are prepared by thermal evaporation technique and they exhibit amorphous structure. Different vibrational modes, observed in infrared spectra of the powder and thin films, were assigned to the molecular bonding structure of PHDMC compound. The optical properties of PHDMC thin films are investigated by measuring the optical transmittance and reflectance at the normal incidence of the light in the spectral range 200–2500 nm. The refractive and absorption indices of the films are found to be independent of the film thickness range mentioned above. The refractive index is analyzed and the dispersion parameters are extracted. Analysis of the absorption coefficient spectra showed that the films have two major indirect allowed electronic transitions; the corresponding optical band gaps are estimated as 2.1 and 3.2 eV in the framework of electronic band-to-band transition theory. The direct current electrical conductivity measurements showed the semiconductor property of the films.

© 2012 Elsevier B.V. All rights reserved.

1. Introduction

Promising chemical and physical properties of organic thin films provide a route that open up avenues for a variety of industrial applications. They have been used as active layers in several electronic and optoelectronic devices such as solar cells [1], Schottky junctions [2], light emitting diodes [3] and optical data storage [4] due to their advantages of low cost, tenability of electronic properties via chemical synthesis and ease of device fabrication. The titled compound belongs to the class of hydrazones. Hydrazones are known as one of the most important classes of organic compounds, some of which have semiconductor properties [5].

They have been used as optical sensors [6] and have been investigated for dye sensitized solar cell applications [7]. A class of hole transporting hydrazones have been studied as new optoelectronic materials [8].

Due to the emergence of organic materials in advanced applications, there is considerable interest in the search for new optical and semiconductor materials. Information concerning the electrical and optical properties of organic thin films as well as their structure relationship would be very important tool in determination the area of application. There are several parameters which control the optical properties of organic layers [9,10]. The film thickness can be considered as a key factor for designing advanced devices. Some studies showed that the optical properties of organic thin films are independent on film thickness, while others are dependent. For instance, El-Nahass and Youssef [11] have reported

* Corresponding author. Tel.: +20 1006021326; fax: +20 233709310.

E-mail address: emad_elmenyawy@yahoo.com (E.M. El-Menyawy).

that the refractive and absorption indices of asymmetrically substituted indium phthalocyanine chloride thin films are independent of thickness range 105–350 nm, while Yakuphanoglu et al. [12] pointed out that the optical constants of Cr(III) complex having 2-pyridine carbaldehyde thiosemicarbazone films are governed by their thickness (33–500 nm). On the other hand, electrical conductivity and its temperature dependence can be used to determine the nature of materials and to characterize the conduction process under application of an electrical field [13].

In this work, 5-(2-phenylhydrazono)-3,3-dimethylcyclohexanone (PHDMC) is synthesized. PHDMC thin films are prepared by using thermal evaporation technique. The X-ray diffraction and Fourier transforms infrared spectra are studied in both powder and thin film forms. The optical properties of thin films are investigated in terms of the spectrophotometric measurements of the transmittance and reflectance. The refractive and absorption indices and their related parameters are determined and analyzed. The electrical conductivity of the films is measured on planar samples.

2. Experimental procedures and optical constants determination

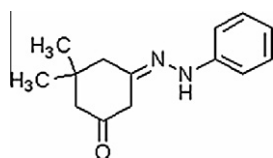
2.1. Synthesis of organic compound

Chemical reagents were commercially available and used without further purification. A solution of 5,5-dimethylcyclohexane-1,3-dione (0.01 mol) was stirred with 2-phenylhydrazine (0.01 mol) in a cold water for an hour. The product was collected by filtration and re-crystallized from acetone to give 5-(2-phenylhydrazono)-3,3-dimethylcyclohexanone (PHDMC) as red crystals in yield 85%, melting point, m.p. 164–166 °C. The molecular structure of PHDMC compound is shown in Scheme 1.

2.2. Thin film preparation and measurements

A high vacuum coating unit (Edwards Model E 306 A, England) was used to prepare PHDMC thin films with different thickness values onto different substrates maintained at room temperature. The vacuum chamber was pumped down to about 5×10^{-4} Pa. The films were vacuum deposited from the powder by using a quartz crucible source heated gradually by a molybdenum boat. The film thickness and deposition rate were monitored and controlled during deposition by using a quartz crystal thickness monitor (Model TM-350 MAXTEK, Inc., USA). The deposition rate was controlled at 3.5–4 Å/s. A mechanical shutter, fixed near to the evaporation source, was used to avoid any probable contamination of the substrates in the initial stage of evaporation and to control roughly the thickness of films. After vacuum breaking, the film thickness was determined from spectral transmittance curve using the interference fringes [14].

Fourier transforms infrared spectra were recorded on ATI Mattson (infinity series FTIR) infrared spectrophotometer in spectral range 400–4000 cm^{-1} . The measurements were carried out for the as-synthesized PHDMC powder mixed with vacuum dried



Scheme 1. Molecular structure of PHDMC compound.

grade KBr, whereas the measurements of thin films were achieved for films deposited on rectangular KBr single crystal substrates.

X-ray diffraction patterns of PHDMC in powder form and in thin film form of thickness 1.247 μm (deposited onto quartz substrates) were recorded on X-ray diffractometer (Philips X'pert) with Ni-filtered $\text{Cu K}\alpha$ -radiation ($\lambda = 1.5418 \text{ \AA}$) in the range of diffraction angle (4–55°). The applied voltage and the tube current were 40 kV and 30 mA, respectively.

The transmittance of PHDMC thin films was measured at the normal incidence of the light in the spectral range 200–2500 nm by using a double beam spectrophotometer (JASCO model V-570 UV-VIS-NIR). The spectrophotometer was also provided with a reflectance unit in order to measure the reflectance in the same spectral range. The films in this experiment were deposited onto optical flat quartz substrates. The structural and optical measurements have been performed on the samples at room temperature (300 K).

Direct current electrical resistance, R , of PHDMC thin films was measured on planar samples by using high impedance electrometer (Keithley 617). The conductivity of the organic material was calculated from the sample dimensions through the relation; $\sigma_{\text{DC}} = L/Rwd$, where L is the distance between the two electrodes, w is the width of the film and d is the film thickness. The ohmic electrodes were made from gold. The gold electrodes were deposited on the two ends of the film by using high vacuum coating unit mentioned above.

2.3. Optical constants determination

The absolute values of total measured transmittance, T , and reflectance, R , after introducing corrections resulting from the absorbance and reflectance of the substrate are calculated by [15]:

$$T = \frac{I_{ft}}{I_q} (1 - R_q), \quad (1)$$

and

$$R = \frac{I_{fr}}{I_m} R_m [(1 - R_q)^2 + 1] - T^2 R_q, \quad (2)$$

where I_{ft} , I_q , I_{fr} , I_m are the intensities of light passing through film-substrate system, reference quartz substrate, light reflected from the sample and light reflected from the reference aluminum mirror, respectively. R_q and R_m are the reflectance of reference quartz substrate and the reflectance of the mirror, respectively.

Different computational methods [16–19] have been used to get the refractive index, n , and absorption index, k , of thin films deposited onto thick non-absorbing substrates. They comprise computer software intended to solve equations relating that constants with spectrophotometric measurements of T and R measured at normal incidence of light. For calculating n and k of films, a modification bidifference search technique of Bennett and Booty [16] has been used in this work. A computer program is used to minimize simultaneously the difference between the calculated values and the experimental ones of both transmittance and reflectance as:

$$(\Delta T)^2 = |T_{\text{cal}} - T|^2 \approx 0 \quad (3)$$

and

$$(\Delta R)^2 = |R_{\text{cal}} - R|^2 \approx 0 \quad (4)$$

where T and R are the experimentally determined values calculated from Eqs. (1) and (2), respectively. T_{cal} and R_{cal} are the calculated values using Murmann's exact equations [20]. The experimental errors are taken into account as follows: $\pm 2.2\%$ for film thickness measurements, $\pm 1\%$ for T and R calculations, $\pm 3\%$ for refractive index and $\pm 2.5\%$ for absorption index computations [21].

3. Results and discussion

3.1. X-ray diffraction

The X-ray diffraction spectra of PHDMC in both as-synthesized powder and as-deposited thin film (1.247 μm) are shown in Fig. 1. PHDMC powder spectra exhibit different peaks with different intensities indicating polycrystalline nature. Films deposited at room temperature show an amorphous structure without any characteristics of the crystallinity judged from XRD measurements. The amorphous nature of as-deposited PHDMC films is primarily attributed to the low adatom mobility due to the low film deposition temperature, where the adatoms on the growing film surface are not activated enough to find the crystalline lattice sites.

The diffraction peaks in powder spectra are indexed and the lattice parameters are determined with the aid of CRYSFIRE computer program [22]. The values of interplanar spacing, d , and Miller indices, hkl , for each diffraction peak before and after refinement are determined by using CHEKCELL program [23]. The values of d and corresponding hkl for PHDMC are listed in Table 1. The results show that PHDMC has a monoclinic crystal structure with space group $P2_1/a$. The lattice parameters are estimated as: $a = 19.932 \text{ \AA}$, $b = 18.869 \text{ \AA}$, $c = 13.095 \text{ \AA}$, $\alpha = \gamma = 90^\circ$ and $\beta = 91.5^\circ$.

3.2. Fourier transforms infrared

Fourier transforms infrared, FTIR, transmittance spectra of PHDMC compound in both powder and thin film (150 nm) forms are demonstrated in Fig. 2. The results show several absorption bands; the important IR characteristic absorption bands, along with their proposed assignments, are summarized in Table 2. The spectrum of PHDMC powder shows two absorption signals at 3246 and 3214 cm^{-1} which are due to asymmetric and symmetric N–H stretching vibrations, respectively. The two bands of weak intensity at 3088 and 3022 cm^{-1} are corresponding to asymmetric and symmetric stretching vibrations of the aromatic C–H bonds, respectively. The vibrations at 2964 cm^{-1} can be attributed to the asymmetric stretching vibration of aliphatic C–H bonds, whereas the 2922 cm^{-1} vibration may arise from the resonance of CH_3 . The vibration at 1602 cm^{-1} is due to the conjugation of the aromatic ring. The band observed at 1546 cm^{-1} reflects the presence of C=N bond. Generally, the functionality in the molecular system made by FTIR spectra (Fig. 1 and Table 1) agrees well with the proposed chemical structure of PHDMC compound given in Scheme 1. On the other hand, the broad band observed around high energies (at 3437 cm^{-1} for powder and at 3442 cm^{-1} for thin film) is due to

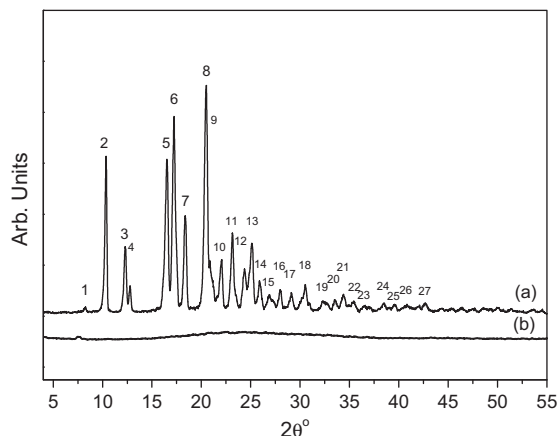


Fig. 1. XRD patterns for PHDMC (a) powder and (b) thin film.

Table 1
Crystallographic data for PHDMC compound.

Peak no.	d_{obs} (\AA)	$2\theta_{\text{obs}}$ ($^\circ$)	$2\theta_{\text{cal}}$ ($^\circ$)	(hkl)
1	10.82843	8.190	8.221	011
2	8.586035	10.350	10.374	$\bar{1}20$
3	6.951989	12.280	12.239	211
4	6.968023	12.790	12.923	$\bar{2}20$
5	5.428059	16.510	16.484	022
6	5.204754	17.240	17.171	122
7	4.892065	18.380	18.421	$\bar{4}10$
8	4.404671	20.500	20.481	$\bar{3}31$
9	4.32799	20.880	20.895	013
10	4.105357	22.070	22.024	$\bar{1}03$
11	3.923641	23.150	23.127	$\bar{3}40$
12	3.738321	24.370	24.382	223
13	3.632276	25.130	25.143	$\bar{1}33$
14	3.532684	25.890	25.918	323
15	3.40704	26.920	26.915	512
16	3.282417	28.030	28.027	$\bar{3}33$
17	3.16972	29.120	29.119	243
18	3.035595	30.540	30.528	261
19	2.888023	32.283	32.305	361
20	2.79395	33.510	33.493	414
21	2.730223	34.400	34.410	353
22	2.660005	35.442	35.448	731
23	2.586275	36.613	36.654	462
24	2.478606	38.485	38.491	325
25	2.420947	39.578	39.594	415
26	2.361191	40.787	40.807	634
27	2.274523	42.698	42.688	921

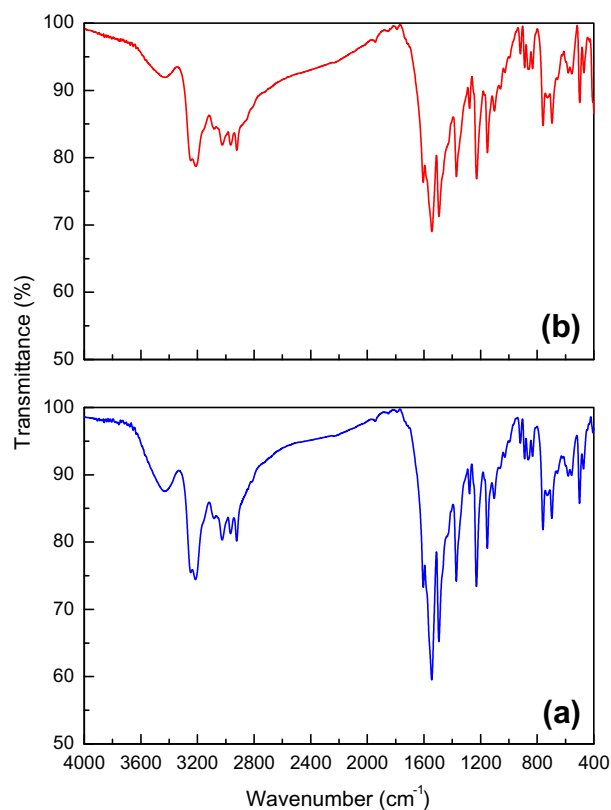


Fig. 2. FTIR spectra for PHDMC: (a) powder and (b) thin film.

–OH group vibrations which can be assigned to hydroxyl group of water; probably water vapors are absorbed from the air atmosphere by potassium bromide and/or the organic material itself. The symmetric absorption bands in powder and thin films indicate

Table 2
Assignment of the important bonds in PHDMC compound.

Wavenumber (cm ⁻¹)		Assignment
Powder	Thin film	
3437	3442	$\nu(\text{OH})$
3246	3234	$\nu(\text{NH})$ as
3214	3210	$\nu(\text{NH})$ s
3088	3089	$\nu(\text{CH})$ as (Ar)
3022	3025	$\nu(\text{CH})$ s (Ar)
2964	2968	as (C–H) aliphatic
2922	2921	$\nu(\text{CH}_3)$
1602	1603	C=C (Ar)
1546	1543	C=N
1493	1495	δ as(CH ₃)
1372	1370	δ s(CH ₃)
1228	1226	$\nu(\text{C–N})$
1151	1150	(CH ₃) wagging
758	757	(CH ₃) rocking
693	695	$\gamma(\text{CH})$ (Ar)
501	498	C–C in plane bending

that the thermal evaporation technique is a suitable one for obtaining undissociated PHDMC films. Obviously, the intensity of absorption bands in powder form is stronger than that of thin film form which can be ascribed to the abundance of the material used.

3.3. Optical constants of thin films

Fig. 3 illustrates the optical transmittance and reflectance of PHDMC thin films as a function of light wavelength, λ . At $\lambda \geq 600$ nm, the total sum of the transmittance and the reflectance nearly equals to unity, indicating an optical transparent region. At $\lambda < 600$ nm, the total sum of the transmittance and the reflectance is less than unity implying optical absorption region. The films have two transmittance edges centered at about 345 and 515 nm. The oscillations observed in transmittance and reflectance spectra arise from the interference effect due to reflectance from the top surface of the film and reflectance at the interface between the film and substrate. The systematic oscillating behavior indicates that the films are homogenous and have flat surface [9].

The optical properties of different materials can be fully characterized by the complex dielectric constant or the complex refractive index, n^* , where $n^* = n + ik$. In general, the real part, n , is related to the dispersion, while the imaginary part, k , provides a measure of dissipation rate of the electromagnetic wave in the dielectric medium. The values of refractive and absorption indices

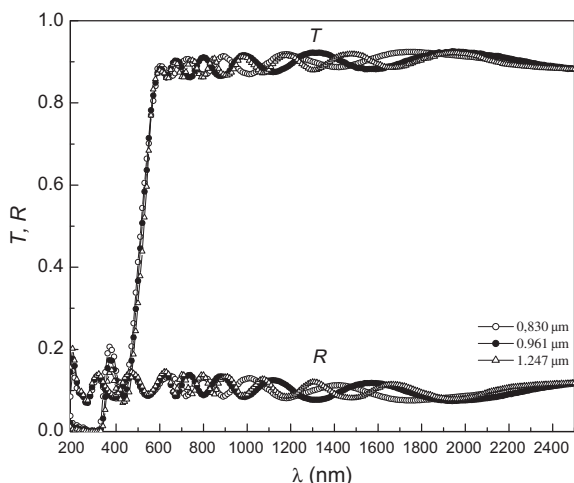


Fig. 3. Transmittance and reflectance spectra for PHDMC thin films.

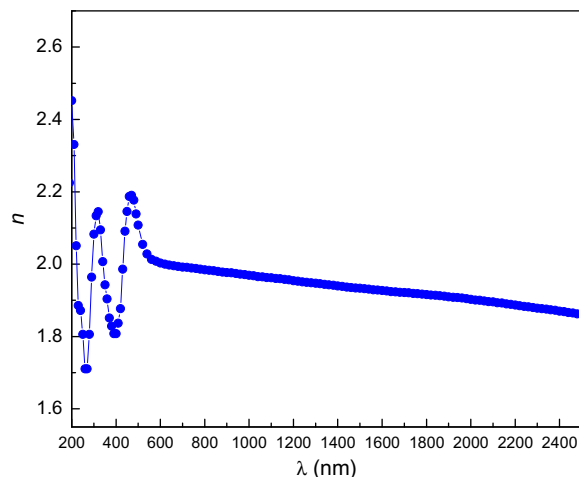


Fig. 4. Refractive index dispersion curve for PHDMC thin films.

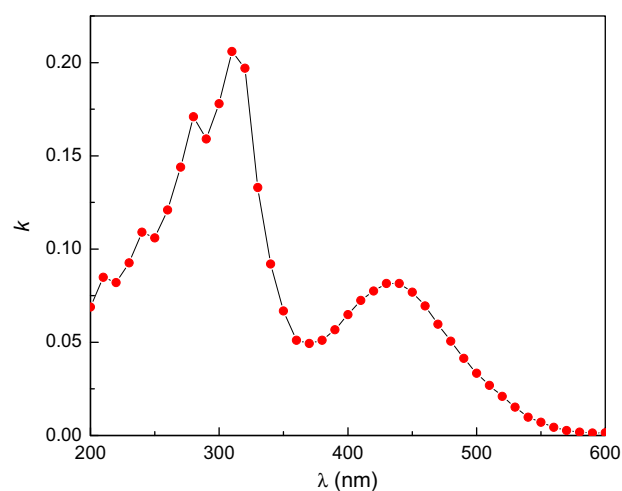


Fig. 5. Absorption index spectrum of PHDMC thin films.

for PHDMC thin films are computed using the absolute values of transmittance and reflectance as mentioned in Section 2.3. The results of calculations show that n and k are independent of film thickness range 0.83–1.247 μm ; therefore, the results depicted in Figs. 4 and 5 represent the average values of n and k for the above mentioned thickness range at wavelength range 200–2500 nm. The independency of the optical constant (n and k) on film thickness is in accordance with the literature for different organic films [24–27]. For the tested films, the films are of amorphous structure and thickness values are large enough as optical properties are independent on their thickness.

The refractive index behavior of PHDMC films in spectral range 200–600 nm represents the anomalous dispersion which can be explained by the multi-oscillator model [28], in which the refractive index shows two peaks with maxima at the wavelength values of 315 and 465 nm and one shoulder at the wavelength value of 245 nm. In general, an optical medium can have many characteristic resonant frequencies (multi-oscillators). The resonances can be attributed to the lattice vibrations in the infrared region and to the oscillations of the bound electrons of the atoms in the ultraviolet and visible regions. In a medium with many electronic oscillators of different frequencies, the total polarization is proportional to the dielectric constant and consequently anomalous dispersion of the refractive index arises in the absorbing region due to electronic

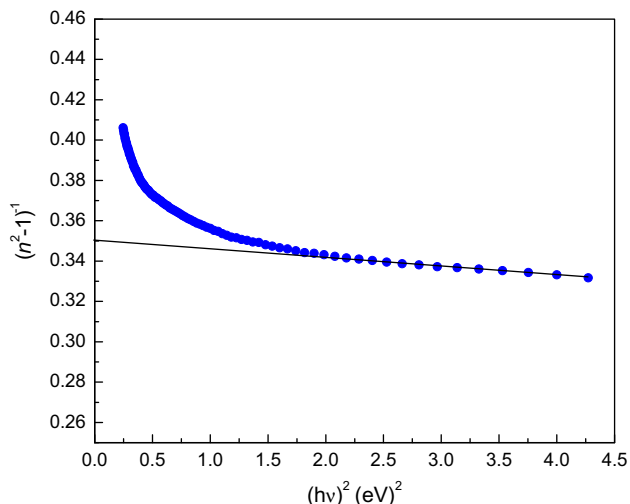


Fig. 6. The variation of $(n^2-1)^{-1}$ with square photon energy for PHDMC thin films.

transitions between any two atomic states [29]. In non-absorbing region and as a result of polarization, the dipoles oscillate nearly with the same frequency (single oscillator). In the wavelength range 600–2500 nm, the refractive index decreases with increasing wavelength showing a normal dispersion. The normal dispersion behavior is analyzed on the basis of the single oscillator model modified by Wemple and DiDomenico [30]. According to this model, the refractive index is expressed as

$$n^2 = 1 + \frac{E_d E_o}{E_o^2 - (hv)^2}, \quad (5)$$

where E_d and E_o are the dispersion and oscillator energies, respectively, and hv is the incident photon energy. The parameter E_d is a measure of the intensity of electronic inter-band transitions and it does not depend significantly on the band gap or the density of the valence electrons; however, E_o can be considered as the average value of the single oscillator energy. An experimental verification of the above equation can be obtained by plotting $(n^2-1)^{-1}$ versus square photon energy for PHDMC films as represented in Fig. 6. The values of the dispersion parameters E_d and E_o as well as the dielectric constants at high frequency, $\epsilon_\infty = n_\infty^2$, are calculated as 25.75 eV, 9.01 eV and 3.86 eV, respectively.

The absorption index spectra of PHDMC films (Fig. 5) exhibit four absorption peaks in ultraviolet region (210, 240, 280 and 314 nm) and one peak in the visible region (435 nm). The absorption peaks are attributed to the electronic transitions across $\pi-\pi^*$ orbitals. At wavelengths greater than 600 nm, there is no absorption at all.

The absorption coefficient, α , of the films is calculated from the well-known equation:

$$\alpha = \frac{2\omega}{c}k \quad (6)$$

where ω is the angular frequency and c is the velocity of light. The absorption coefficient as a function of photon energy for PHDMC thin films is depicted in Fig. 7. The films show high absorption coefficient value, as it is in the order of 10^5 cm^{-1} . The absorption coefficient curve includes two major absorption edges indicating the presence of two main optical transitions occurring in such films.

Analysis of the absorption coefficient spectra near the threshold energy is a standard method for determining the type of electronic inter-band transition and evaluating the optical band gap of different crystalline and amorphous non-metallic materials. The

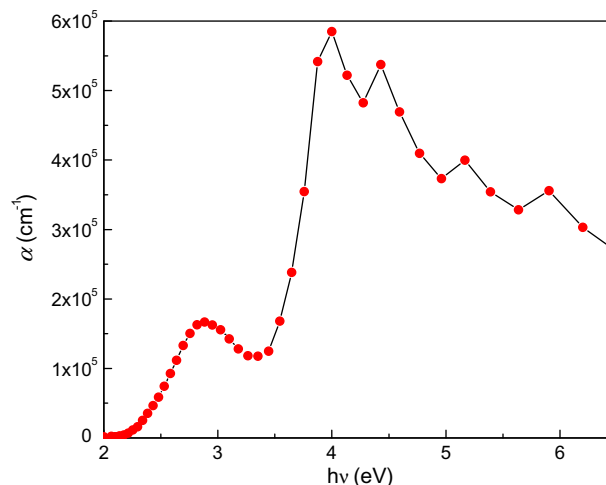


Fig. 7. Spectral dependence of absorption coefficient, α , on hv for PHDMC thin films.

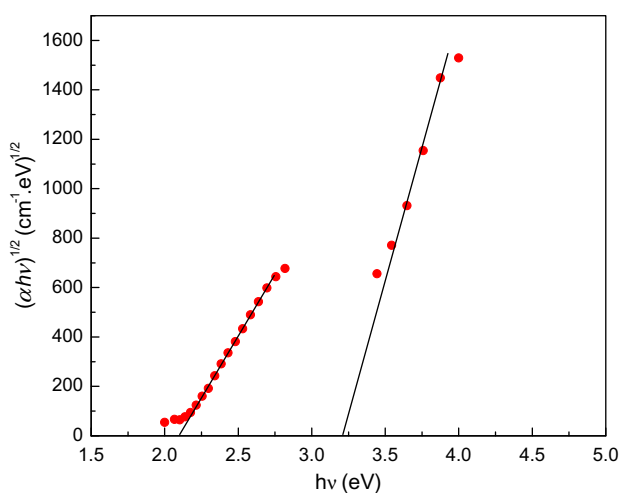


Fig. 8. Relation between $(\alpha hv)^{1/2}$ and hv for PHDMC thin films.

dependence of the absorption coefficient on the photon energy can be expressed as [31]

$$\alpha hv = B(hv - E_g)^m \quad (7)$$

where $m = 1/2$ and $3/2$ for direct allowed and forbidden transitions, respectively; $m = 2$ and 3 for indirect allowed and forbidden transitions, respectively, hv is photon energy, E_g is the optical band gap and B is a parameter depending on transition probability. The variation of absorption coefficient with incident photon energy was plotted for both the direct and indirect transitions. The plot of $(\alpha hv)^{1/2}$ versus hv shown in Fig. 8 is found to have the best straight line fit which supports the interpretation of indirect allowed transition rather than the other types of transitions. The values of E_g are obtained by extrapolating the straight lines to $(\alpha hv)^{1/2} = 0$. The optical band gaps of PHDMC thin films are estimated as 2.1 and 3.2 eV for the onset and the fundamental absorption edges, respectively. The observed indirect allowed transition is in accordance with amorphous structure of the films [32].

From Fig. 7, it can be seen that the absorption coefficient shows a tail before reaching zero value. Fig. 9 demonstrates the semi-logarithmic plot of the absorption coefficient versus the photon energy. The relationship is linear verifying the Urbach's empirical equation [33]

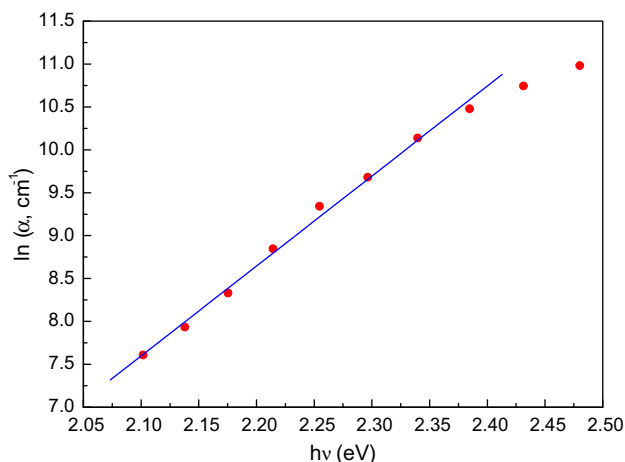


Fig. 9. Urbach's relation for PHDMC thin films.

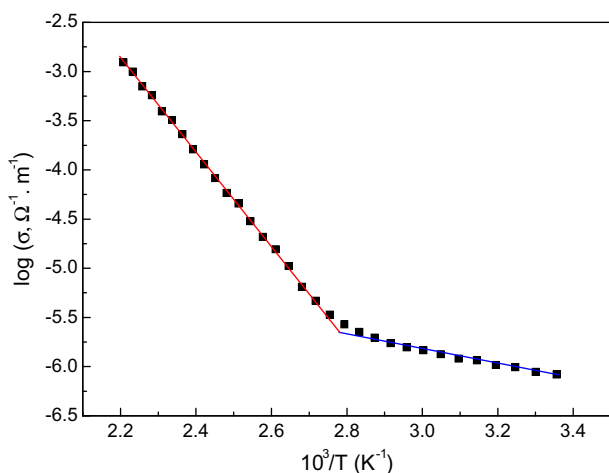


Fig. 10. Temperature dependence of PHDMC conductivity.

$$\alpha = \alpha_0 \exp\left(\frac{hv}{E_u}\right), \quad (8)$$

where α_0 is a constant that depends on the material and E_u is the Urbach energy which is an indicator of structural disorder. The value of E_u is estimated from the slope of the straight line as 95 meV.

3.4. Electrical conductivity

The room temperature conductivity of PHDMC films is found to be 6.52×10^{-7} , 8.31×10^{-7} and $9.95 \times 10^{-7} \Omega^{-1} \text{m}^{-1}$ for film thickness values 0.83, 0.961 and 1.247 μm , respectively. The conductivity seems to increase with increasing film thickness, but it is being in the same order of magnitude. Fig. 10 depicts the logarithm of conductivity versus $10^3/T$ for PHDMC film with a thickness of 0.961 μm . The conductivity increases with rising heating temperature indicating semiconductor behavior. The results show two straight lines with different slopes. In semiconductor materials, conduction mechanisms depend on several parameters such as the degree of crystallinity, thermal excitation, impurities, lattice defects and temperature [34]. The conductivity of the compound can be described by Arrhenius equation given by:

$$\sigma = \sigma_1 \exp\left(\frac{-\Delta E_1}{k_B T}\right) + \sigma_2 \exp\left(\frac{-\Delta E_2}{k_B T}\right) \quad (9)$$

where ΔE_1 and ΔE_2 are the activation energy at low and relatively high temperatures, respectively, σ_1 and σ_2 are constants, k_B is the Boltzmann's constant and T is the absolute temperature. According to Eq. (9), as the temperature is increased, more charge carriers overcome the activation energy barrier and participate in the electrical conduction. The values of ΔE_1 and ΔE_2 are estimated as 0.16 and 0.95 eV, respectively. The magnitude of ΔE_2 is nearly half the optical band gap that obtained at the onset of the absorption (2.1 eV). This indicates that the conduction in this region is due to intrinsic process [35]. Referring to the activation energy estimated at lower temperatures (E_1), the conduction in this region can be ascribed to the extrinsic process [35], in which the activation energy is needed to excite the carriers from the corresponding trap levels to the conduction band.

4. Summary and conclusions

5-(2-Phenylhydrazono)-3,3-dimethylcyclohexanone (PHDMC) powder is chemically synthesized in polycrystalline structure with monoclinic space group, $P2_1/a$. The lattice parameters are determined as: $a = 19.932 \text{ \AA}$, $b = 18.869 \text{ \AA}$, $c = 13.095 \text{ \AA}$, $\alpha = \gamma = 90^\circ$ and $\beta = 91.5^\circ$. Thermally evaporated PHDMC thin films exhibited amorphous structure. Fourier transforms infrared indicated that the thermal evaporation is a suitable technique for obtaining PHDMC thin films. The refractive and absorption indices of the films are found to be independent of film thickness range 0.83–1.247 μm . The dispersion of the refractive index follows the single oscillator model, from which the dispersion energy, oscillator energy and dielectric constant at high frequency are estimated as 25.75 eV, 9.01 eV and 3.86, respectively. The films exhibit absorption coefficient in the order of 10^5 cm^{-1} , with two indirect allowed transitions and the corresponding optical band gaps are determined as 2.1 and 3.2 eV. From the electrical conductivity measurements, it has shown that the compound under investigation is an organic semiconductor with calculated electronic parameters such as room temperature conductivity and activation energy.

References

- [1] X. Zhang, L. Mao, D. Zhang, L. Zhang, J. Mol. Struct. 1022 (2012) 153.
- [2] M.M. El-Nahass, K.F. Abd El-Rahman, J. Alloy. Compd. 430 (2007) 194.
- [3] M. Guan, L. Li, G. Cao, Y. Zhang, B. Wang, X. Chu, Z. Zhu, Y. Zeng, Org. Electron. 12 (2011) 2090.
- [4] S. Tsutomu, M. Shohji, U. Yasunobu, T. Tatsuya, S. Noboru, H. Yasuhiro, US Patent No. 6197477, 06, March, 2001.
- [5] H.B. Hassib, Y.M. Issa, W.S. Mohamed, J. Therm. Anal. Calorim. 92 (2008) 775.
- [6] M. Bakir, I. Hassan, T. Johnson, O. Brown, O. Green, C. Gyles, M.D. Coley, J. Mol. Struct. 688 (2004) 213.
- [7] A.G. Al-Sehemi, A. Irfan, A.M. Asiri, Y.A. Ammar, J. Mol. Struct. 1019 (2012) 130.
- [8] F.-F. Tian, F.-L. Jiang, X.-L. Han, C. Xiang, Y.-S. Ge, J.-H. Li, Y. Zhang, R. Li, X.-L. Ding, Y. Liu, J. Phys. Chem. B. 114 (2010) 14842.
- [9] H.M. Zeyada, M.M. El-Nahass, I.K. El-Zawawi, E.M. El-Menyawy, J. Phys. Chem. Solids 71 (2010) 867.
- [10] N.A. El-Ghamaz, A.Z. El-Sonbati, Sh.M. Morgan, J. Mol. Struct. 1027 (2012) 92.
- [11] M.M. El-Nahass, T.E.J. Youssef, Luminescence 31 (2011) 1419.
- [12] F. Yakuphanoglu, M. Sekerci, A. Balaban, Opt. Mater. 27 (2005) 369.
- [13] H.M. Zeyada, M.M. El-Nahass, Appl. Surf. Sci. 254 (2008) 1852.
- [14] J.C. Manificier, M. De Murcia, J.P. Fillard, Thin Solid Films 41 (1977) 127.
- [15] M.M. El-Nahass, E.M. El-Menyawy, Mater. Sci. Eng., B 177 (2012) 145.
- [16] H.E. Bennett, M.J. Booty, Appl. Opt. 5 (1966) 41.
- [17] P.O. Nilson, Appl. Opt. 7 (1968) 432.
- [18] F. Abélés, M.L. Théyé, Surf. Sci. 5 (1966) 325.
- [19] H.E. Bennett, M.J. Booty, Phys. Thin Films 4 (1967) 31.
- [20] O.S. Heavens, in: G. Hass, R. Thus (Eds.), Phys. Thin Films, Academic, New York, 1964, p. 193.
- [21] I. Konstantinov, T. Babeva, S. Kitova, Appl. Opt. 37 (17) (1998) 4260.
- [22] R. Shirley, The CRYSFIRE System for Automatic Powder Indexing: User's Manual, The Lattice Press, Guildford, Surrey GU2 7NL, England, 2000.
- [23] J. Laugier, B. Bochu, LMGP-suite suite of programs for the interpretation of X-ray experiments, ENSP/Laboratoire des Matériaux et du Génie Physique, BP46.38042, Saint Martin d'Heres, France, 2000.
- [24] M.M. El-Nahass, H.M. Zeyada, M.S. Aziz, N.A. El-Ghamaz, Opt. Mater. 27 (2004) 491.
- [25] M.M. El-Nahass, A.A.M. Farag, A.A. Atta, H.A. Ali, Synth. Met. 159 (2009) 589.

- [26] M.M. El-Nahass, A.A. Atta, H.E.A. El-Sayed, E.F.M. El-Zaidia, *Appl. Surf. Sci.* 254 (2008) 2458.
- [27] H.M. Zeyada, M.M. El-Nahass, S.A. Samak, *J. Non-Cryst. Solids* 358 (2012) 915.
- [28] A. Stendal, U. Beckers, S. Wilbrand, O. Stenzel, C. Von Borczys-kowski, *J. Phys. B: At. Mol. Opt. Phys.* 29 (1996) 2589.
- [29] M. Fox, *Optical Properties of Solids*, Oxford University Press, 2001.
- [30] S.H. Wemple, M. DiDomenico, *Phys. Rev. B* 3 (1970) 1338.
- [31] J. Tauc, A. Menth, *J. Non-Cryst. Solids* 8–10 (1972) 569.
- [32] A.S. Maan, D.R. Goyal, *J. Non-Cryst. Solids* 183 (1995) 186.
- [33] F. Urbach, *Phys. Rev.* 92 (1953) 1324.
- [34] M.S. Refat, M.A.A. Moussa, S.F. Mohamed, *J. Mol. Struct.* 994 (2011) 194.
- [35] M.M. El-Nahass, K.F. Abd-El-Rahman, A.A.A. Darwish, *Phys. B* 403 (2008) 219.